Trees (2008) 22:449–462
DOI 10.1007/s00468-007-0205-4

ORIGINAL PAPER

Photosynthetic induction in leaves of co-occurring *Fagus lucida* and *Castanopsis lamontii* saplings grown in contrasting light environments

Kun-dong Bai · De-bao Liao · De-bing Jiang · Kun-fang Cao

Received: 20 September 2006 / Revised: 26 November 2007 / Accepted: 13 December 2007 / Published online: 8 February 2008

Abstract Photosynthetic induction times and photoinhibition in relation to simulated sunflecks (sudden increase of irradiance from 20 to 1,500 μmol m^{-2} s^{-1}) were examined in leaves of co-occurring *Fagus lucida* (a deciduous tree) and *Castanopsis lamontii* (an evergreen tree) saplings grown either in a beech forest understory or in an adjacent open site during a late rainy season. Two hypotheses were tested: (1) understory leaves would display faster photosynthetic induction times and greater photoinhibition than open-grown leaves; and (2) evergreen species would have slower photosynthetic induction times and lighter photoinhibition than deciduous species. Times to reach 90% of maximal CO_2 assimilation rate ($t_{90\%A}$) and stomatal conductance ($t_{90\%g_s}$) did not differ between species, but showed faster by 3–5 min in open-grown leaves than understory leaves due to higher initial stomatal conductance ($g_{s\ initial}$) and induction state 1 min into simulated sunflecks (IS_{1min}) in the former. Our analysis across the published data on photosynthetic induction of 48 broad-leaved woody species again revealed the negative correlations between $t_{90\%A}$ and either $g_{s\ initial}$ or IS_{1min}, and the similarity of $t_{90\%A}$ and $t_{90\%g_s}$ between evergreen and deciduous species. Measurements of maximum PSII photochemical efficiency (F_v/F_m) indicated that photoinhibition occurred in saplings in any of the growth habitats during sunfleck-induced photosynthetic induction. Despite no interspecific differences in the degree of photoinhibition, understory leaves of both species suffered heavier photoinhibition than open-grown leaves, as indicated by a stronger decrease of F_v/F_m in the former. Dynamic changes in the quantum yields of PSII photochemistry and ΔpH- and xanthophyll-regulated thermal dissipation and adjustments in the partitioning of electron flow between assimilative and non-assimilative processes were functional to resist photoinhibition. However, such photoinhibition, together with stomatal and biochemical limitations, would decrease carbon gain during simulated sunflecks, particularly in understory leaves.

Keywords Photosynthetic induction · *Fagus lucida* · *Castanopsis lamontii* · Photoinhibition · Sunfleck

Communicated by R. Matyssek.

K. Bai · K. Cao (✉)
Xishuangbanna Tropical Botanical Garden,
Chinese Academy of Sciences,
Kunming 650223, Yunnan, China
e-mail: caokf@xtbg.ac.cn

K. Bai
Graduate School of Chinese Academy of Sciences,
Beijing 100039, China

D. Liao · D. Jiang
Guangxi Miao'ershan Mountain National Nature Reserve, Guilin
541316, Guangxi Zhuang Autonomous Region, China

Introduction

Plants growing in the understory of closed forests are exposed to low diffuse light punctuated by intense sunflecks that may last from seconds to minutes (Pearcy 1983; Chazdon and Fetcher 1984). It was estimated that sunflecks might account for 10–80% of the total irradiance and result in 30–60% of total daily carbon gain for understory plants (Pearcy 1987; Chazdon 1988; Pearcy 1990). Understory plants are assumed to display faster induction responses to sunflecks than gap or open-grown plants because of this relative importance of sunflecks for daily carbon gain (e.g., Leakey et al. 2005; Tausz et al. 2005). However, the mixed results, with some studies reporting faster photosynthetic induction in understory plants (Küppers and Schneider 1993; Tang et al. 1994) and others reporting similar or slower induction responses (similar, e.g., Kursar and Coley 1993 and Rijkers et al. 2000; slower, e.g., Han et al. 1999 and Tausz et al. 2005), suggest that the issue whether growth light environment affects sunfleck-induced photosynthetic induction is still on debate.

On the other hand, lots of papers have addressed the interspecific differences in response to sunflecks (e.g., species differing in life form or light requirement) (e.g., Ögren and Sundin 1996; Rijkers et al. 2000). However, to our knowledge, little attention has been paid to the comparison of evergreen and deciduous woody species in relation to sunflecks. A study on some tropical evergreen woody species differing in leaf lifespan showed that species with long-lived leaves tended to have slower induction responses to sunflecks because of their longer activation of Rubisco activity (Kursar and Coley 1993). Then, the question whether deciduous woody species tend to respond faster to sunflecks than evergreen woody species due to their shorter leaf longevity, arises.

Although sunflecks are important sources of light energy for understory plants, they may have some harmful effects because of the time lag between the start of a sunfleck illumination and the achievement of maximal CO_2 assimilation rate (c.f., Tausz et al. 2005). Due to Rubisco deactivation, the small pool sizes of Calvin cycle intermediates and the low degree of stomatal openings at the beginning of a sunfleck (Kirschbaum and Pearcy 1988; Stegemann et al. 1999), this time-lag leads to the quantum of absorbed light energy being, at least temporarily, in excess of what is used in photochemistry and results in photoinhibition (Logan et al. 1997; Watling et al. 1997; Tausz et al. 2005). However, inter- and intra-specific differences in photoinhibition imposed by sudden exposure to high light can vary. Some studies suggested that understory plants were more susceptible to photoinhibition during sunflecks because they displayed lower photosynthetic capacity and the smaller pool size of xanthophyll-cycle components than gap or open-grown plants (Logan et al. 1997; Watling et al. 1997; Tausz et al. 2005). Lovelock et al. (1998) suggested that species with short-lived leaves displayed greater photoinhibition than the species with long-lived leaves due to their lower yield of PS II photochemistry. If these results apply in the case of the comparison between deciduous and evergreen woody species, would deciduous woody species experience heavier photoinhibition when exposed to sudden high light, or, understory plants of both kinds of species display greater photoinhibition during sunflecks than gap and open-grown plants?

Fagus lucida, a climax tree species with leaf lifespan of less than 7 months, is a dominant species in some forests of the montane zones in subtropical China (Cao et al. 1995). *Castanopsis lamontii*, with leaf longevity of about 15 months, co-dominates in some beech forests. Both species are shade tolerant and able to regenerate in the forest understory (Cao et al. 1995; Cao 2001). In this paper, we report gas exchange and photoinhibition in response to simulated sunflecks in *F. lucida* and *C. lamontii*. As previous studies on sunfleck responses focused mainly on emerging understory plants in comparison with gap plants (e.g., Poorter and Oberbauer 1993; Allen and Pearcy 2000; Cao and Booth 2001), we made measurements on current mature leaves of saplings in the understory and in an adjacent open site. The coordinated changes in stomatal opening, photochemical efficiency, photorespiration, CO_2 assimilation and water use efficiency (WUE) during sunflecks were analyzed to test the following hypotheses: (1) understory leaves would display faster photosynthetic induction times and greater photoinhibition than open-grown leaves; (2) evergreen species would exhibit slower photosynthetic induction times and lighter photoinhibition than deciduous species.

Materials and methods

Study site and sample trees

The study was conducted in a mixed beech forest located on the southern slope of Miao'ershan Mountain (25°50′N, 110°49′E, and c.1,500 masl) in the Guangxi Zhuang Autonomous Region, China. This mountain, with the highest peak of 2142.5 masl, is a part of Nanling Mountain Range that partially blocks the cold winds coming from northern China in winter. Mean annual air temperature recorded by the weather station at 1,200 masl is 12.8°C, with mean monthly temperature ranging from 2.9 °C in January to 21.8°C in July. Mean annual precipitation is 2,509 mm. The forest stand where we carried out the study is dominated by *F. lucida*, mixed with evergreen tree species such as *C. lamontii* and *Lithocarpus hancei* (Cao 2001).

In early September (late rainy season) 2005, measurements were made on current mature leaves of three *F. lucida* or *C. lamontii* saplings growing both in the forest understory and in an adjacent open site. Sapling height ranged from 1.0 to 3.0 m. The sampled saplings received daily cumulative photosynthetic photon flux density (PPFD) of 3.42 ± 0.94 mol m^{-2} day^{-1} in the understory and 50.26 ± 2.35 mol m^{-2} day^{-1} in the open site, based on the means (±SD) of two quantum sensors (LI-190SA, LICOR, Lincoln, NE, USA) for each site recording at 1-min intervals on three clear days. Background PPFD in the understory was less than 50 μmol m^{-2} s^{-1} during most of the daytime with several sunflecks (maximal sunfleck PPFD close to 1,500 μmol m^{-2} s^{-1}) occurring at midday.

Gas exchange and chlorophyll fluorescence

Measurements of leaf gas exchange and chlorophyll fluorescence were made on overcast days to ensure that the leaves were evenly acclimated to low irradiance prior to all measurements. Photosynthetic CO_2 and light response curves were determined on understory and open-grown leaves using a portable infrared gas analyzer (Li-6400, LICOR, Lincoln, NE, USA). Photosynthetic CO_2 response curves (A–c_i curves) were made at a saturating PPFD of 1,500 μmol m^{-2} s^{-1}. Leaf temperature was controlled at 20 ± 1°C and leaf-to-air vapor pressure deficit was less than 1.0 kPa. Leaves were exposed to 380 μmol mol^{-1} CO_2 in air and a PPFD of 1,500 μmol m^{-2} s^{-1} until CO_2 assimilation rate (A) and stomatal conductance (g_s) were steady (after a minimum of 10 min). Afterward, the response of A to the changes in intercellular CO_2 concentration (c_i) was by decreasing the ambient CO_2 in the air (c_a) passing over the leaves in nine intervals ranging from 1,500 to 50 μmol m^{-2} s^{-1}; moreover, photosynthesis was allowed to stabilize for at least 3 min at each c_a. The CO_2 response of photosynthesis was fitted to an empirical nonlinear model described by Liu and Robert (1995).

Photosynthetic light response curves were measured under the same chamber conditions as A–c_i curves, except that chamber CO_2 concentration was kept at 380 μmol mol^{-1} and PPFD was allowed to vary. Leaves were enclosed in the dark chamber and dark respiration was recorded once the rates of gas exchange were steady. And then, PPFD was increased stepwise to a maximum of 2,000 μmol m^{-2} s^{-1}. Measurements were logged once rates of gas exchange were stable, which took 5–15 min at each point depending on the preceding conditions. The light response of photosynthesis was fitted to the Mitscherlich function (Peek et al. 2002). The Mitscherlich function was a nonlinear function: $A = A_{max}[1 - e^{-AQY(PPFD-LCP)}]$ where A_{max} represents the asymptote of photosynthesis at high light, AQY corresponds to the initial slope of the curve at low light levels and LCP denotes the x-intercept where net photosynthesis is equal to 0, and A is net photosynthesis, the response variable.

Dynamic state gas exchange was obtained using the time-lamped program of the Li-6400. Leaves were sealed in the leaf chamber at a PPFD of 20 μmol m^{-2} s^{-1}, and steady-state A and g_s were recorded for 2 min once the reading was stable. Thereafter, PPFD was increased to 1,500 μmol m^{-2} s^{-1} in one step and rates of gas exchange were logged at 2-s intervals for 20 min. During the whole duration of the simulated dynamic light response, leaf temperature was controlled around 20°C. The induction of A, g_s and WUE, calculated as A/g_s; Knapp and Smith 1989) to the sudden increase in PPFD were fitted to the following equations:

$$A_{(t)} = A_{initial} + (A_{max} - A_{initial}) \cdot (1 - e^{-t/t1})$$

$$WUE_{(t)} = WUE_{initial} + (WUE_{max} - WUE_{initial}) \cdot (1 - e^{-t/t1})$$

$$g_{s(t)} = g_{s\,initial} + (g_{s\,max} - g_{s\,initial})/[1 + (t/t1)^p]$$

where $A_{initial}$, $g_{s\ initial}$ and $WUE_{initial}$ are the initial A, g_s and WUE in low light (20 μmol m^{-2} s^{-1}), A_{max}, $g_{s\ max}$ and WUE_{max} are their maximal values at fully induction, *t1* is a characteristic time constant and p is a parameter determining the curve shape. Before these equations were fitted, some induction data points showing manyfold higher or lower than their neighboring data points within every 1 min (due to unavoidable noise when taking the Li-6400 IRGAs measurements so frequently) were removed. Several parameters were then calculated using the resulting curve equations: A_{1min} (A at 1 min into simulated sunflecks), $t_{90\%A}$ (time to reach 90% of A_{max}), IS_{1min} (induction state 1 min into simulated sunflecks calculated as A_{1min}/A_{max}), $t_{90\%g_s}$ (time to reach 90% of $g_{s\ max}$) and $t_{90\%WUE}$ (time to reach 90% of WUE_{max}).

Chlorophyll fluorescence was measured following the procedures of Tausz et al. (2005), with a fluorometer (FMS 2, Hansatech, Norfolk, UK). Maximal photochemical efficiency of PSII ($F_v/F_{m\ initial}$) was determined after 10 min dark adaptation; this dark adaptation time proved long enough to restore PSII maximal photochemical efficiency, because all leaves had been pre-adapted to low light during the cloudy measurement days. Then, leaves were allowed to stabilize at a PPFD of 20 μmol m^{-2} s^{-1} and the florescence level before the saturation pulse (F_s) and the maximum florescence during the saturation pulse (F_m') were determined. Following the course of photosynthetic induction, F_s and F_m' were determined at 1–1.5 min intervals. When the 20-min simulated sunfleck ended, leaves were dark-adapted for 10 min and F_v/F_m was determined again ($F_v/F_{m\ 20min}$). In order to estimate the partitioning of absorbed light between photochemistry and thermal dissipation during simulated sunflecks, leaves were tagged and predawn maximum fluorescence (F_m) were measured in the next morning when maximum closure of all PSII reaction center traps occurred. According to Hendrickson et al. (2004), the allocation of photons absorbed by the PSII antennae to photochemical electron transport and thermal dissipation could be assessed in unity by defining and parameterizing the quantum efficiencies of photochemistry (Φ_{PSII}, calculated as $1 - F_s/F_m'$), ΔpH- and xanthophyll-regulated thermal dissipation (Φ_{NPQ}, calculated as $F_s/F_m' - F_s/F_m$) and the sum of fluorescence (Φ_F) and constitutive (Φ_D) thermal dissipation (Φ_{FD}, calculated as F_s/F_m). By the way, this method of light energy allocation estimation was proved to give very similar results to the method proposed by Kramer et al. (2004) (see details in Hendrickson et al. 2004).

Compared with Kramer et al.'s method, the advantage of Hendrickson et al.'s method is that it does not require the measurements of dark-adapted and light-adapted minimal fluorescence (F_0 and F_0', respectively). During sunfleck-induced photosynthetic induction, F_s and F_m' could be detected easily while F_0 and F_0' measurements were difficult to perform; furthermore, the losses of F_0 and F_0' measurements could help minimize the effects of light beam generated from fluorescence analyzer on leaf dynamic physiology. Finally, according to Valentini et al. (1995), photorespiration (R_p) during the course of photosynthetic induction was also estimated by combining the time-dependent induction curves of A and electron transport rate (ETR, calculated as Φ_PSII·PPFD·0.5·0.84). Ideally, such calculations of PSII quantum efficiencies and R_p would require F_s, F_m', A and ETR to be measured under steady-state conditions. Because of the time-lag effect during simulated sunflecks, steady-state conditions may not have been achieved before full induction. However, such parameters are still considered as valuable indicators for reflecting the dynamic physiological changes from non-steady to steady-state (e.g., Kursar and Coley 1993; Logan et al. 1997; Watling et al. 1997; Han et al. 1999; Schulte et al. 2003;Tausz et al. 2005).

Statistical analysis

We tested the differences between species and the effect of growth light environment on each variable by two-way ANOVAs (species and light as source factors) with Type III sums of squares. Previously, ANCOVA was explored considering sapling height as covariable; sapling height did not significantly affect the variables examined ($P > 0.05$ in all cases; therefore, we present here only the ANOVA results for simplicity). A similar two-way ANOVA was used to explore the differences between the evergreen and deciduous broad-leaved woody species listed in Appendix Table 4, using leaf phenology as the factor instead of species. Before ANCOVA and ANOVA, data were square-rooted or log-transformed to meet the assumptions of homogeneity of variance and normality (Zar 1984). Linear regression analyses were used to test for precise relationships between pairs of variables. All statistical analyses were performed using SPSS version 12.0 for Windows.

Results

Steady-state gas exchange

In both *F. lucida* and *C. lamontii*, sapling height did not have significant impact on the study steady-state gas exchange traits, as well as the dynamic traits (data not shown). However, there were large differences between open-grown and understory leaves in their steady-state light- and CO_2-responses (Fig. 1). Open-grown leaves had almost twofold higher A_max and R_d than understory leaves ($P > 0.001$), but there was little difference in AQY (mean $= 0.032$, $P = 0.719$). The initial slope of the A–c_i curve and A at high c_i were also greater in open-grown leaves than understory leaves ($P < 0.001$). However, no significantly interspecific differences in these parameters were found in open-grown or understory leaves ($P > 0.1$).

Responses of gas exchange and chlorophyll fluorescence to simulated sunflecks

When PPFD was increased from 20 to 1,500 μmol $\mathrm{m}^{-2}\ \mathrm{s}^{-1}$, the time courses of photosynthetic induction in both open-grown and understory leaves of the two species resembled a sigmoidal increase in stomatal opening and a hyperbolic

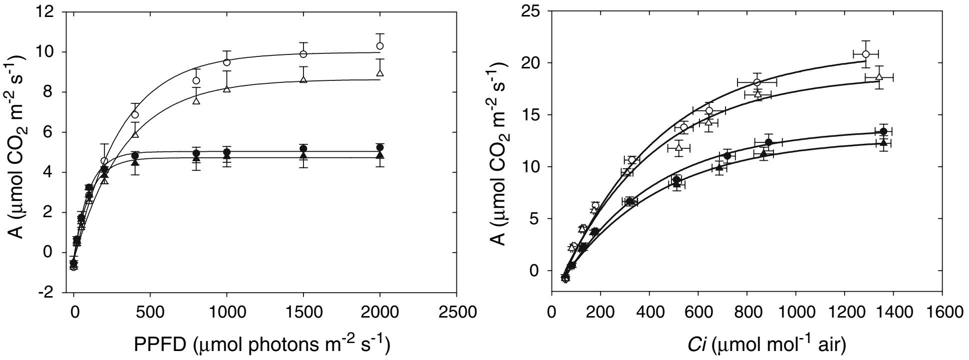

Fig. 1 Steady-state photosynthesis in leaves of open-grown (*open symbols*) and understory saplings (*closed symbols*) of *Fagus lucida* (*circles*) and *Castanopsis lamontii* (*triangles*) in a montane mixed beech forest. **a** The response of CO_2 assimilation rate (A) to incident PPFD. The light-response curve was fitted to the Mitscherlich function. **b** The response of CO_2 assimilation rate (A) to internal CO_2 concentration (c_i). The A–c_i curve was fitted to an empirical nonlinear function. *Error bars* are standard deviations of three leaves from three different individuals

response in A, WUE, ETR or R_p (Figs. 2, 3). The hyperbolic response was characterized by a rapid increase in A, WUE, ETR or R_p to 50–80% and an obvious drop in c_i. In the sigmoidal response, stomatal opening occurred in two phases, an initial slow phase followed by a gradual rise to the steady-state.

Open-grown leaves had significantly higher $A_{1\text{min}}$ and $\text{IS}_{1\text{min}}$ and faster $t_{90\%A}$ and $t_{90\%g_s}$ than understory leaves, whereas interspecific differences in these parameters were not significant (Table 1). In addition, $t_{90\%\text{WUE}}$, $t_{90\%\text{ETR}}$ and $t_{90\%R_p}$ varied little between open-grown and understory leaves, although large differences in WUE_{max}, ETR_{max} and $R_{\text{p max}}$ were found between leaves of the two habitats (Table 1). Also, $t_{90\%\text{WUE}}$, $t_{90\%\text{ETR}}$ and $t_{90\%R_p}$ did not differ significantly between species, whereas they were 3–5 min faster than $t_{90\%A}$ in respective habitats (Table 1).

To separate stomatal and biochemical limitations during photosynthetic induction, A was plotted as a function of c_i. For both species, as the responses of A to c_i in open-grown leaves were similar in shape to those in understory leaves, only responses of the latter are shown for clarity (Fig. 4). Photosynthetic induction of *C. lamontii* was characterized by a sudden initial decrease in c_i caused by light-activated biochemical components of photosynthetic apparatus and slow opening of stomata and a subsequent increase in c_i due to decreasing stomatal limitation. Photosynthetic induction of *F. lucida* showed a constantly slow decrease in c_i until A reached the steady-state A–c_i curve, suggesting no difference in time span between the removals of stomatal and biochemical limitation.

Open-grown leaves had lower $F_v/F_{m\text{ initial}}$ than understory leaves for both species, without interspecific differences in each habitat. Upon illumination with 20-min simulated sunflecks, F_v/F_m in both species strongly decreased, with even stronger decrease in the understory leaves than in open-grown leaves, whereas no interspecific differences in the decrease of F_v/F_m in each habitat were found (Table 2). Both open-grown and understory leaves of the two species generally showed Φ_{PSII} to decrease rapidly to the minimum and increase slowly thereafter, Φ_{NPQ} to increase fast to the maximum and drop slowly to the steady-state and Φ_{FD} to remain almost constant (Fig. 3 and Table 2). However, open-grown leaves allocated more absorbed light to Φ_{PSII} during photosynthetic induction than understory leaves, which in turn partitioned more absorbed light toΦ_{NPQ}. But, no interspecific differences in the allocation of absorbed light were found. Moreover, a tight linear relationship between the quantum yields of Φ_{PSII} and Φ_{NPQ} was found irrespective of the species and growth light environments ($\Phi_{\text{PSII}} + \Phi_{\text{NPQ}} = 0.8$), indicating that decrease in the efficiency of PSII photochemistry was compensated by proportional increase in non-photochemical processes related to photoprotection.

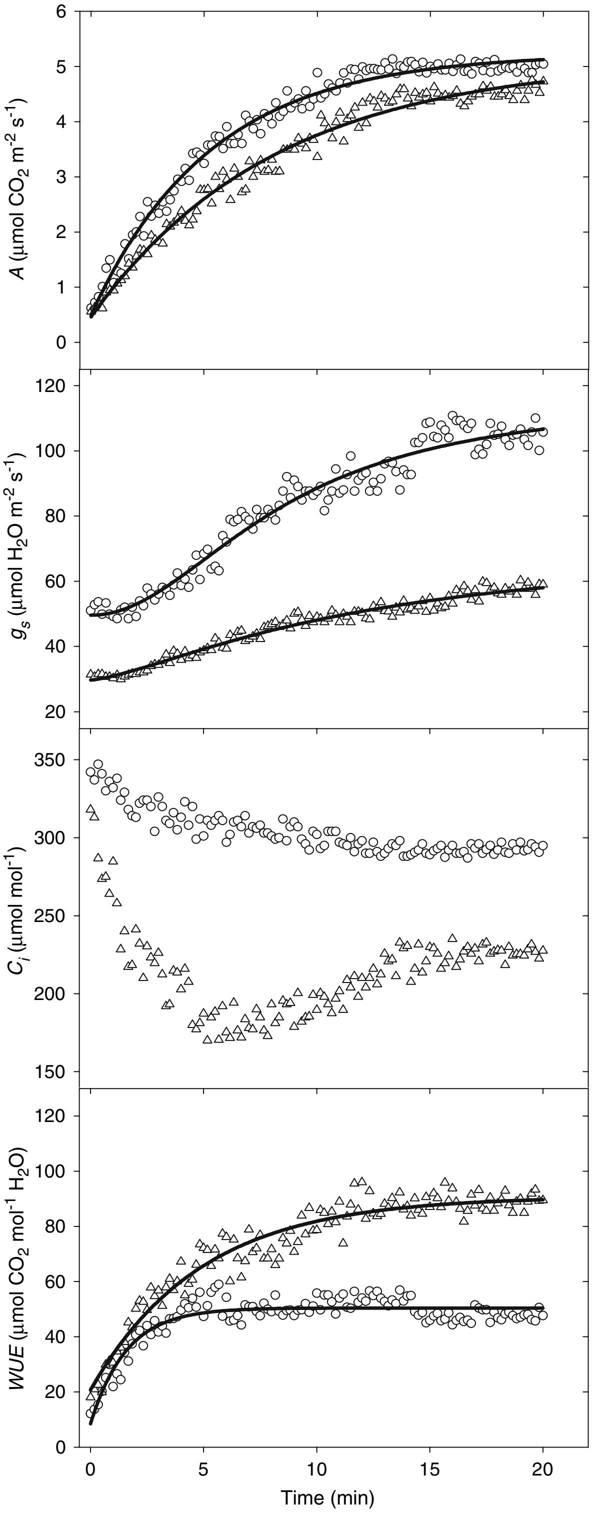

Fig. 2 The representative time course of CO$_2$ assimilation rate (A), stomatal conductance (g_s), intercellular CO$_2$ concentration (c_i) and water use efficiency (*WUE*) during photosynthetic induction in understory leaves of *Fagus lucida* (*circles*) and *Castanopsis lamontii* (*triangles*). For clarity, only every fifth to tenth data points collected are plotted. *Solid lines* indicate fitted functions (exponential for A and WUE, and logistic for g_s)

Fig. 3 Responses of the allocation of absorbed light energy to photochemistry of photosystem II (Φ_{PSII}), ΔpH- and xanthophyll-regulated thermal dissipation (Φ_{NPQ}) and the sum of fluorescence and constitutive thermal dissipation (Φ_{FD}), and electron transport rate (*ETR*) and photorespiratory CO_2 production (R_p) in understory leaves of *Fagus lucida* (*circles*) and *Castanopsis lamontii* (*triangles*) to simulated sunflecks. ETR and R_p curves were fitted to exponential functions similar to *A* and WUE

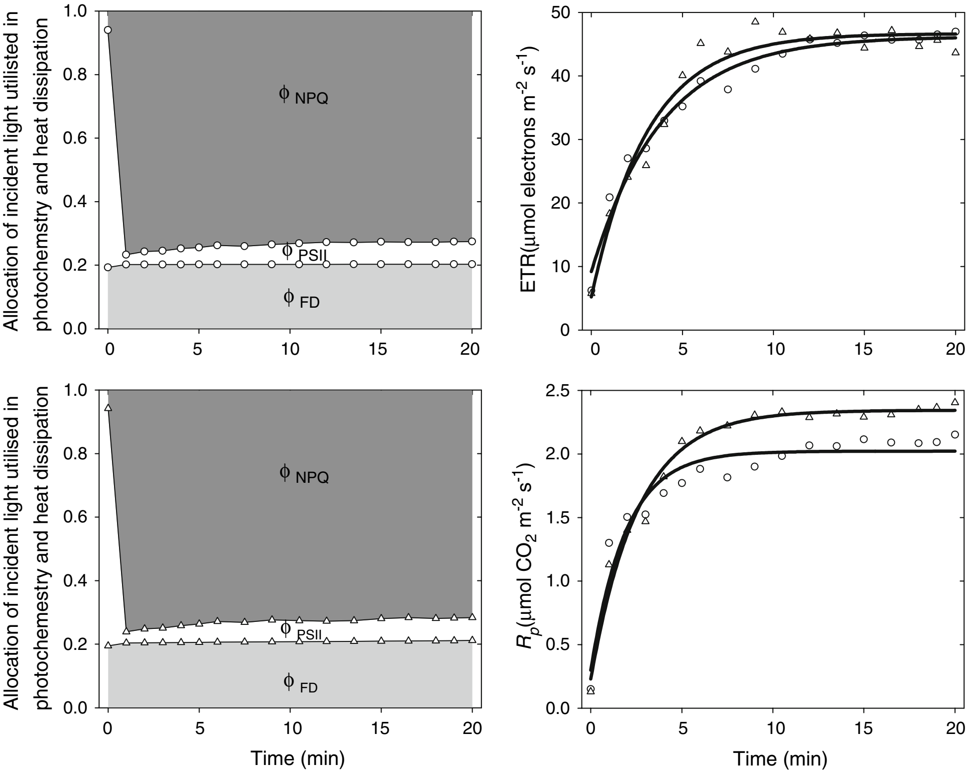

Table 1 The characteristics of photosynthetic induction in open-grown and understory leaves of *Fagus lucida* and *Castanopsis lamontii*

	Open		Understory		*P*-values		
	F. lucida	*C. lamontii*	*F. lucida*	*C. lamontii*	Light	Species	Interaction
$A_{initial}$ (μmolCO_2 m^{-2} s^{-1})	0.46 ± 0.08	0.36 ± 0.05	0.62 ± 0.08	0.55 ± 0.07	0.002	0.068	0.745
A_{max} (μmolCO_2 m^{-2} s^{-1})	9.65 ± 0.47	8.69 ± 1.19	5.13 ± 0.15	4.71 ± 0.31	<0.001	0.109	0.499
A_{1min} (μmolCO_2 m^{-2} s^{-1})	2.48 ± 0.32	2.09 ± 0.30	1.10 ± 0.14	0.95 ± 0.06	<0.001	0.080	0.382
IS_{1min} (%)	25.6 ± 2.1	24.1 ± 1.4	21.3 ± 2.0	20.3 ± 1.5	0.005	0.245	0.818
$t_{90\%\ A}$ (min)	8.05 ± 1.45	8.98 ± 1.37	11.09 ± 1.24	12.44 ± 3.27	0.024	0.356	0.862
$g_{s\ initial}$ (mmol $H_2O$$m^{-2}$ s^{-1})	146.5 ± 10.5	81.8 ± 7.1	49.8 ± 2.2	31.4 ± 2.5	<0.001	<0.001	<0.001
$g_{s\ max}$ (mmol $H_2O$$m^{-2}$ s^{-1})	272.5 ± 12.8	132.5 ± 7.7	110.1 ± 9.6	61.3 ± 3.5	<0.001	<0.001	<0.001
$t_{90\%g_s}$ (min)	10.47 ± 1.80	14.28 ± 2.49	14.81 ± 2.42	17.05 ± 2.87	0.035	0.063	0.593
$WUE_{initial}$ (μCO_2 mol^{-1} H_2O)	3.52 ± 0.74	4.13 ± 0.53	13.02 ± 1.57	18.91 ± 1.15	<0.001	0.001	0.003
WUE_{max} (μCO_2 mol^{-1} H_2O)	35.63 ± 2.41	69.10 ± 3.65	47.54 ± 4.01	78.85 ± 4.50	<0.001	0.001	0.629
$t_{90\%WUE}$ (min)	4.60 ± 1.12	4.74 ± 0.71	3.91 ± 1.48	4.49 ± 0.69	0.461	0.572	0.726
$ETR_{initial}$ (μmol m^{-2} s^{-1})	6.19 ± 0.12	6.22 ± 0.13	6.25 ± 0.16	6.26 ± 0.10	0.428	0.893	0.893
ETR_{max} (μmol m^{-2} s^{-1})	71.89 ± 6.66	68.50 ± 6.34	35.89 ± 4.18	41.92 ± 4.72	<0.001	0.694	0.182
$t_{90\%ETR}$ (min)	4.64 ± 0.38	4.99 ± 0.33	4.21 ± 0.51	4.91 ± 0.38	0.053	0.309	0.472
$R_{p\ initial}$ (μmol CO_2 m^{-2} s^{-1})	0.12 ± 0.03	0.11 ± 0.02	0.15 ± 0.02	0.13 ± 0.03	0.124	0.188	0.599
$R_{p\ max}$ (μmol CO_2 m^{-2} s^{-1})	3.34 ± 0.22	3.09 ± 0.16	2.14 ± 0.14	2.38 ± 0.23	<0.001	0.954	0.059
$t_{90\%R_p}$ (min)	4.88 ± 1.13	5.12 ± 0.75	4.32 ± 1.15	4.89 ± 0.42	0.480	0.470	0.762

Values are means ± SD of three leaves from three different individuals

Estimation of carbon balance in photosynthetic induction

In both species, the estimated total amount of CO_2 assimilation during a 20-min sunfleck of 1,500 μmol m^{-2} s^{-1} was higher in open-grown leaves compared with understory leaves, but this varied little between species in each habitat (Table 3). Neglecting the stomatal, biochemical and photoinhibitory limitations (i.e., assuming an immediate realization of A_{max} with PPFD at 1,500 μmol m^{-2} s^{-1})

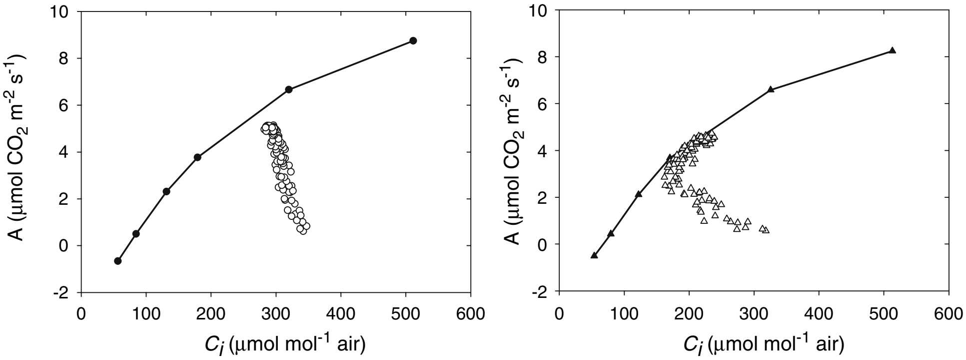

Fig. 4 The representative responses of net photosynthesis (A) to intercellular CO_2 concentration (c_i) from the steady-state gas exchange (*closed symbols*) and photosynthetic induction (*open symbols*) measurements in understory leaves of *Fagus lucida* (*circles*) and *Castanopsis lamontii* (*triangles*) in a montane mixed beech forest

Table 2 Responses of chlorophyll fluorescence parameters in open-grown and understory leaves of *Fagus lucida* and *Castanopsis lamontii* to simulated sunflecks

	Open		Understory		*P*-values		
	F. lucida	*C. lamontii*	*F. lucida*	*C. lamontii*	Light	Species	Interaction
$F_v/F_{m\ \mathrm{initial}}$	0.747 ± 0.004	0.745 ± 0.005	0.762 ± 0.004	0.757 ± 0.005	0.001	0.247	0.632
$F_v/F_{m\ \mathrm{20min}}$	0.516 ± 0.002	0.512 ± 0.004	0.365 ± 0.003	0.363 ± 0.003	<0.001	0.188	0.825
$\Phi_{\mathrm{FD\ initial}}$	0.220 ± 0.010	0.221 ± 0.008	0.195 ± 0.003	0.193 ± 0.003	<0.001	0.901	0.710
$\Phi_{\mathrm{NPQ\ initial}}$	0.042 ± 0.005	0.051 ± 0.003	0.060 ± 0.004	0.062 ± 0.008	0.001	0.115	0.301
$\Phi_{\mathrm{PSII\ initial}}$	0.738 ± 0.015	0.740 ± 0.016	0.745 ± 0.003	0.745 ± 0.011	0.428	0.893	0.892
$\Phi_{\mathrm{FD\ 1min}}$	0.220 ± 0.009	0.227 ± 0.010	0.202 ± 0.002	0.203 ± 0.008	0.002	0.419	0.632
$\Phi_{\mathrm{NPQ\ 1min}}$	0.732 ± 0.012	0.729 ± 0.011	0.763 ± 0.005	0.766 ± 0.008	<0.001	0.975	0.603
$\Phi_{\mathrm{PSII\ 1min}}$	0.047 ± 0.014	0.044 ± 0.003	0.035 ± 0.003	0.030 ± 0.002	<0.001	0.084	0.635
$\Phi_{\mathrm{FD\ 20min}}$	0.226 ± 0.009	0.225 ± 0.011	0.207 ± 0.011	0.212 ± 0.010	0.034	0.731	0.617
$\Phi_{\mathrm{NPQ\ 20min}}$	0.647 ± 0.014	0.653 ± 0.009	0.716 ± 0.008	0.716 ± 0.007	<0.001	0.597	0.635
$\Phi_{\mathrm{PSII\ 20min}}$	0.127 ± 0.005	0.125 ± 0.003	0.074 ± 0.002	0.071 ± 0.002	<0.001	0.335	0.787

Values are means ± SD of three leaves from three different individuals

Table 3 Modeled assimilative and non-assimilative carbon balance in open-grown and understory leaves of *Fagus lucida* and *Castanopsis lamontii* to simulated sunflecks

	Open		Understory	
Assimilative (mmol CO_2 m^{-2})				
Assuming immediate induction	11.58	122%	6.16	141%
F. lucida	10.43	123%	5.66	136%
C. lamontii				
Using observed induction	9.51	100%	4.38	100%
F. lucida	8.45	100%	4.17	100%
C. lamontii				
Non-assimilative (mmol CO_2 m^{-2})				
R_p	3.41	36%	1.69	39%
F. lucida	3.44	41%	1.76	42%
C. lamontii				

Values are averages of three leaves from three different individuals

would result in an overestimation of CO_2 assimilation during a 20-min sunfleck by 22 and 23% in open-grown leaves and by 41 and 36% in understory leaves for *F. lucida* and *C. lamontii*, respectively. On the other hand, photorespiratory CO_2 production during a 20-min sunfleck was greater in open-grown leaves than in understory leaves for both species. However, there was a strongly positive linear relationship between assimilative and non-assimilative CO_2 production regardless of the species and growth light environments ($\mathrm{Total}_A = 2.5865\mathrm{Total}_{R_p} - 0.03$, $r^2 = 0.877$, $P < 0.001$), showing the delicate carbon balance between assimilative and non-assimilative processes.

Discussion

Photosynthetic acclimation to light environments

Both species exhibited higher values for most gas exchange parameters (e.g., $A_{\max}$, R_d and $g_{s\ \max}$) measured in open-grown leaves than in understory leaves, except for $\mathrm{WUE}_{\max}$ (Fig. 1 and Table 1). These results were consistent with the previous studies showing that sun-adapted leaves had greater $A_{\max}$ at the expense of higher R_d and water loss compared with shade-adapted leaves (e.g., Boardman 1977; Givnish 1988). However, interspecific differences in open-grown or understory leaves were not significant for most gas exchange parameters except for $g_{s\ max}$ and WUE_{max} (Table 1). Deciduous *F. lucida* always had higher $g_{s\ max}$ but lower WUE_{max} than evergreen *C. lamontii* across the light environments. These results showed that the contrasting WUE_{max} between the two species were not attributed to the differences in A_{max} but to $g_{s\ max}$. This was also supported by the findings of many previous studies on higher WUE_{max} in evergreen broad-leaved woody species due to lower $g_{s\ max}$ than deciduous ones (Appendix Table 4; Givnish 2002; Bowman and Prior 2005).

Response of gas exchange to simulated sunflecks

Since understory leaves experienced much more sunflecks than open-grown leaves, we anticipated that the understory leaves would show faster photosynthetic induction following a sudden increase in PPFD. The result was borne out to be the opposite. Times taken to 90% of $g_{s\ max}$ and A_{max} during a simulated sunfleck were slower by 3–5 min in understory leaves than in open-grown leaves of both species (Table 1). This is consistent with the findings of Han et al. and Tausz et al. (Han et al. 1999; Tausz et al. 2005). There are, however, some reports showing faster photosynthetic induction in understory leaves than leaves from more exposed habitats such as gap and open sites (Küppers and Schneider 1993; Tang et al. 1994). On the other hand, many studies showed that photosynthetic induction time was not affected by growth light environment (Roden and Pearcy 1993; Kursar and Coley 1993; Zipperlen and Press 1997; Rijkers et al. 2000). These mixed results might be attributed to too small a collective body of information in a certain research from which to draw general conclusions. Using the data sets from 15 studies (Appendix Table 4), a two-way ANOVA across a wide range of species showed that $t_{90\%A}$ and $t_{90\%g_s}$ were not significantly affected by growth light environment ($P = 0.142$ and 0.052, respectively).

Because of the contrasting leaf longevity between evergreen and deciduous woody plants, we expected that *F. lucida* with lower leaf lifespan would respond faster to sunflecks than *C. lamontii* with higher leaf lifespan on the basis of the study of Kursar and Coley (1993). However, our results rejected this expectation; no significant differences in either $t_{90\%A}$ or $t_{90\%g_s}$ between the two species were found (Table 1). This finding was further confirmed by a two-way ANOVA across a wide range of species in Appendix Table 4 showing no significant differences in $t_{90\%A}$ and $t_{90\%g_s}$ between the evergreen and deciduous broad-leaved woody plants ($P = 0.746$ and 0.534, respectively).

Our data from the two study species showed that those leaves with lower $g_{s\ initial}$ and IS_{1min} tended to require relatively longer $t_{90\%A}$ (Table 1). Furthermore, an analysis across a large data set compiled in Appendix Table 4 again revealed the significantly negative correlation between $t_{90\%A}$ and either $g_{s\ initial}$ or IS_{1min} (Fig. 5). This role of $g_{s\ initial}$ and IS_{1min} in photosynthetic induction was important in that higher $g_{s\ initial}$ and IS_{1min} could improve stomatal opening, alleviate the restriction of CO_2 supply and fasten the Rubisco activation (Valladares et al. 1997; Han et al. 1999; Naramoto et al. 2001). Although in the present study induction loss in the shade after simulated sunflecks was not included, an analysis of the large data set complied in Appendix Table 4 revealed a negative correlation between A_{max} and induction state after 10 min shade (IS_{10min}) (Fig. 5), suggesting that induction loss was mainly regulated by Rubisco activity (Valladares et al. 1997; Naumburg and Ellsworth 2000).

Photoinhibition and photoprotection during simulated sunflecks

Simulated sunflecks caused severer photoinhibition in understory leaves than in open-grown leaves of both species, as indicated by the larger decrease in F_v/F_m during sunflecks in the former (Table 2). This result is consistent with our expectation and previous studies (Logan et al. 1997; Watling et al. 1997; Tausz et al. 2005). However, interspecific differences in photoinhibition during sunflecks were not significant, contrary to our expectation.

A reliable way for a plant to resist photoinhibition is to enable the photosynthetic apparatus to process more photons through photochemistry, thereby decreasing the time spent in the reduced state of Q_A and accelerating CO_2 assimilation. (Öquist et al. 1992; Lovelock et al. 1998). Both species of the present study responded to simulated sunflecks through adjustments in the allocation of light energy to photochemistry, and these adjustments had influence on photosynthetic induction (Tables 1, 2 and Fig. 2). Open-grown leaves allocated more light energy to photochemistry, and thus had lighter photoinhibition and faster photosynthetic induction than understory leaves for both species. Due to no interspecific differences in the allocation of light energy to photochemistry during photosynthetic induction, the degrees of photoinhibition, $t_{90\%A}$ and $t_{90\%g_s}$, were similar in the two species. Interestingly, $t_{90\%ETR}$ and $t_{90\%R_p}$ in both species were achieved about 5 min and more quickly than $t_{90\%A}$, suggesting fast regulations in the allocation of electron flow to photorespiration. Considering an obvious drop in

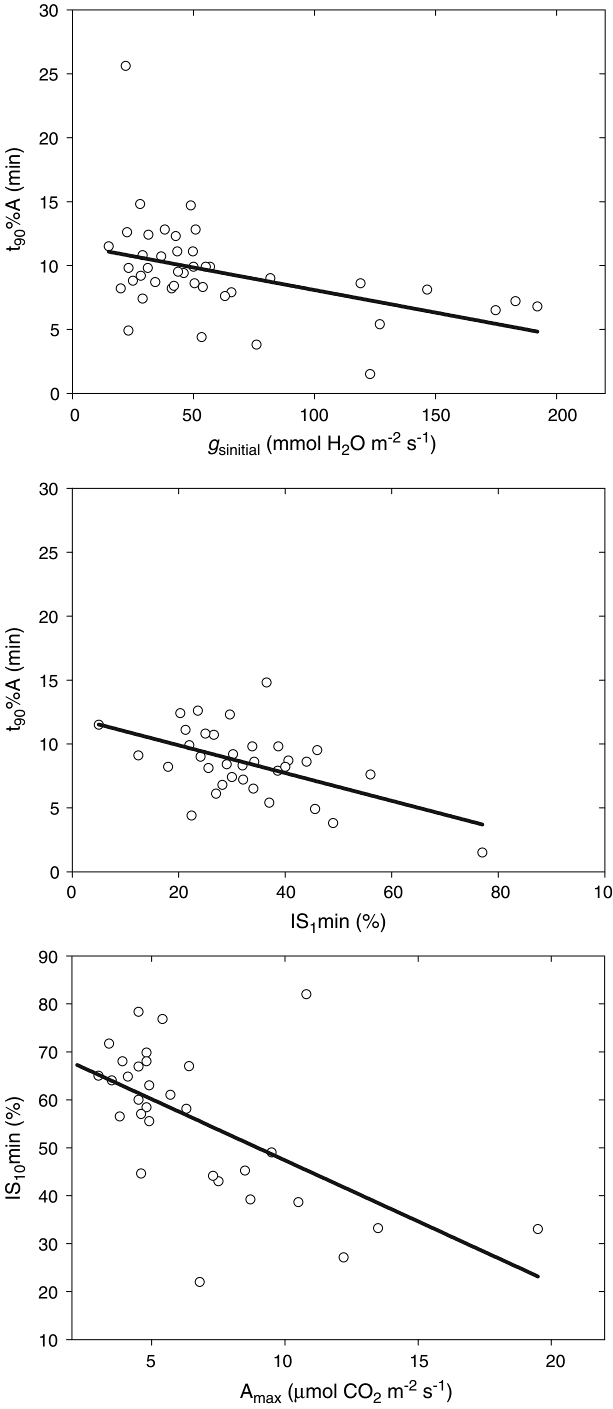

Fig. 5 The correlations between the initial stomatal conductance ($g_{\text{s initial}}$) and induction state 1 min into simulated sunflecks (IS_{1min}), and time to reach 90% of maximum CO_2 assimilation rate ($t_{90\%A}$), and between induction state after 10 min dark-adaptation (IS_{10min}) and maximum CO_2 assimilation rate (A_{max}) from the large data set compiled in Appendix Table 4. Equations for the regression lines: $t_{90\%A} = 11.612 - 0.035g_{\text{s initial}}$, $n = 42$, $r^2 = 0.185$, $P < 0.01$; $t_{90\%A} = 12.070 - 0.109IS_{1min}$, $n = 35$, $r^2 = 0.275$, $P < 0.01$; $IS_{10min} = 72.851 - 2.547A_{max}$, $n = 31$, $r^2 = 0.354$, $P < 0.001$

c_i during photosynthetic induction, we deduced that fast responses of R_p, along with rapid responses of Φ_{NPQ}, might be a mechanism to compensate for the restriction in CO_2 supply to photosynthesis during a sunfleck. This consideration was also supported by a relative constant ratio of integrated R_p to CO_2 assimilation, being about 0.4 during simulated sunflecks in both species (Table 3). Similarly, it was found that in *Alocasia macrorrhiza* (Kirschbaum and Pearcy 1988) and other tropical rain-forest trees (Kursar and Coley 1993) the induction of O_2 evolution of photosynthesis was parallel to the induction of ETR and exhibited more rapidly than the induction of CO_2 assimilation, indicating adjustments in the allocation of electron flow to oxygenation. This partitioning of electron flow to oxygenation was related to the high specificity of Rubisco to O_2 when the concentration of CO_2 in the chloroplast was low during photosynthetic induction (Kirschbaum and Pearcy 1988; Kursar and Coley 1993). However, some reports have suggested that the Mehler ascorbate peroxidase reaction and water–water cycle could also act as an important sink for light-driven electrons (Osmond and Grace 1995; Kozaki and Takeba 1996; Miyake and Yokota 2001). If this is the case, the contributions of photorespiration and oxygenation to photoprotection might be overestimated. In addition, $t_{90\%\text{WUE}}$ was faster than $t_{90\%A}$ in the two species (Table 1). This faster realization of WUE_{max} has also been found in some other studies and regarded as a mechanism to improve carbon gain (Knapp and Smith 1989; Allen and Pearcy 2000; Schulte et al. 2003).

Stomatal, biochemical and photoinhibitory limitations on carbon gain during simulated sunflecks

During a 20-min sunfleck of 1,500 µmol m^{-2} s^{-1}, the estimated total CO_2 assimilation according to the induction measurement was lower than that predicted by the steady-state model, whereas no interspecific differences were found in open-grown or understory leaves (Table 3). The lower-estimated total CO_2 assimilation was attributed to the stomatal, biochemical and photoinhibitory limitations. These limitations resulted in a loss of CO_2 assimilation during a 20-min sunfleck by 22 and 23% in open-grown leaves and by 41 and 36% in understory leaves for *F. lucida* and *C. lamontii*, respectively. Similar results were reported for *Nothofagus cunninghamii* (Tausz et al. 2005). But, we did not determine the relative contributions of stomatal, biochemical and photoinhibitory limitations to carbon gain during a sunfleck separately, largely due to the concurrent interactions of these limitations and the difficulty to set them apart. However, a recent theoretical study on *N. cunninghamii* suggested that photoinhibition had little effect on carbon gain during a sunfleck (Tausz et al. 2005).

Conclusions

Photosynthetic response of *F. lucida* and *C. lamontii* saplings to sunflecks is partly consistent with our hypothesis that understory leaves of both species display faster photosynthetic times and greater photoinhibition than open-grown leaves. In fact, open-grown leaves displayed faster photosynthetic induction due to higher $g_{s\ \mathrm{initial}}$ and $\mathrm{IS}_{1\mathrm{min}}$, and lighter photoinhibition due to more allocation of absorbed light to photochemistry; moreover, our analysis across the wide range of broad-leaved woody species in the literature indicated that photosynthetic induction time was not significantly affected by growth light environment, but negatively correlated with $g_{s\ \mathrm{initial}}$ and $\mathrm{IS}_{1\mathrm{min}}$. On the other hand, we expected that evergreen *C. lamontii* would have slower photosynthetic induction times and lighter photoinhibition than deciduous *F. lucida* in responses to simulated sunflecks. However, the case was against our expectation. Both species responded similarly to photosynthetic induction and protection from photoinhibition in that they shared identical regulations in Φ_{PSII} and Φ_{NPQ} and adjustments in the partitioning of electron flow between assimilative and non-assimilative processes; furthermore, our analysis across the wide range of broad-leaved woody species in the literature also revealed the similarity of photosynthetic induction times between evergreen and deciduous broad-leaved woody species. Although no interspecific differences in photoinhibition were found between *F. lucida* and *C. lamontii*, such photoinhibition, together with stomatal and biochemical limitations, resulted in the decease of carbon gain during sunflecks, particularly in the understory leaves.

Acknowledgments This work was financially supported by the National Natural Science Foundation of China through a research grant (30670320) to Kun-fang Cao. We thank Jun-jie Zhu and Jun-wen Chen for their technical assistance in the field and useful suggestions on the manuscript. Acknowledgements are extended to two anonymous reviewers who made very helpful comments on the manuscript.

Appendix

Table 4

Table 4 Summary of photosynthetic induction traits in evergreen and deciduous broad-leaved woody species reported in the literature and the present study

Species	Growth environment	$A_{\max}$ (μmol CO_2 m^{-2} s^{-1})	$g_{s\ \mathrm{initial}}$ (mmol H_2O m^{-2} s^{-1})	$g_{s\ \max}$ (mmol H_2O $m^{-2}s^{-1}$)	$\mathrm{WUE}_{\max}$ (μCO_2 mol^{-1} H_2O)	$\mathrm{IS}_{1\mathrm{min}}$ (%)	$t_{90\%A}$ (min)	$t_{90\%g}$ (min)	IS after 10 min shade (%)	Reference
Evergreen										
Alseis blackiana	Ust	2.8					6			Kursar and Coley (1993)
Aspidosperma cruenta	Ust	3.1					12			Kursar and Coley (1993)
Barringtonia pendala	Ust	3.5	34.2	54.5	64.2	40.6	8.7			Cai et al. (2003)
Calophyllum longifolium	Ust	4.7					12			Kursar and Coley (1993)
Castonopsis lamontii	Ust	4.7	31.4	61.3	78.9	20.3	12.4	17.1		Present study
Cornus florida	Ust	4.6	28	78	59.0		14.8	22.4	57^{b}	Naumburg and Ellsworth (2000)
Cotylelobium burckii	Ust	4.9					16.9		55.5	Cao and Booth (2001)
Dicorynia guianensis	Ust	4.3	29	73	58.9	25	10.8			Rijkers et al. (2000)
Dipterocarpus borneensis	Ust	4.8					37.4		69.8	Cao and Booth (2001)
Dipteryx panamensis	Ust	4.5					16.3		60	Poorter and Oberbauer (1993)
Dryobalanops lanceolata	Ust	3.0					21.2	24.7	65	Zipperlen and Press (1997)
Hopea pentanervia	Ust	4.5					25		78.3	Cao and Booth (2001)
Hybanthus prunifolius	Ust	3.4					3			Kursar and Coley (1993)

Table 4 continued

Species	Growth environment	A_{max} (μmol CO_2 m^{-2} s^{-1})	$g_{s\ initial}$ (mmol H_2O m^{-2} s^{-1})	$g_{s\ max}$ (mmol H_2O $m^{-2}s^{-1}$)	WUE_{max} (μCO_2 mol^{-1} H_2O)	IS_{1min} (%)	$t_{90\%A}$ (min)	$t_{90\%g}$ (min)	IS after 10 min shade (%)	Reference
Lasianthus hookeri	Ust	2.2	23.1	52.4	42	45.6	4.9			Cai et al. (2003)
Linociora insignis	Ust	4.2	42.7	84.3	49.8	29.6	12.3			Cai et al. (2003)
Lithocarpus chingtungensis	Ust	4.1	28.3	62.5	64.8	32.2	9.2	11.6	64.8	Unpublished data[a]
Mallotus marcrostachys	Ust	7.2	53.4	170.7	42.2	22.4	4.4			Cai et al. (2003)
Manglietia insignis	Ust	3.8	22.6	70.9	53.7	33.6	12.6	14.3	56.5	Unpublished data[a]
Ouratea lucens	Ust	2.9					13			Kursar and Coley (1993)
Pometia tomentosa	Ust	3.6	23.2	61.3	58.7	38.7	9.8			Cai et al. (2003)
Pourouma bicolor	Ust	4.1	29	96	42.7	30	7.4			Rijkers et al. (2000)
Psychotria acuminata	Ust	3.9	43.6	66.3	58.8	46	9.5		68	Valladares et al. (1997)
Psychotria horzontails	Ust	2.2					5			Kursar and Coley (1993)
Psychotria limonensis	Ust	4.9	50.5	88.1	55.6	44	8.6		63	Valladares et al. (1997)
Psychotria marginata	Ust	4.8	63	94.8	50.6	56	7.6		68	Valladares et al. (1997)
Rheedia edulis	Ust	2.5					37			Kursar and Coley (1993)
Shorea chinesis	Ust	3.8	31.2	71.5	53.2	33.8	9.8			Cai et al. (2003)
Shorea leprosula	Ust	3.5					16	17.8	64	Zipperlen and Press (1997)
Shorea multiflora	Ust	3.4					25.3		71.7	Cao and Booth (2001)
Shorea pachyphyll	Ust	5.4					9.1		76.8	Cao and Booth (2001)
Swartzia simplex	Ust	5.3					12			Kursar and Coley (1993)
Voucapoua Americana	Ust	4.1	20	45	91.1	40	8.2			Rijkers et al. (2000)
Ceropia obtusifolia	Gap	7.5					9.9		43	Poorter and Oberbauer (1993)
Cotylelobium burkii	Gap	8.7							39.2	Cao and Booth (2001)
Dicorynia guianensis	Gap	5.1	41	69	73.9	18	8.2			Rijkers et al. (2000)
Psychotria micrantha	Gap	10.8	53.9	250	43.2	32	8.3		82	Valladares et al. (1997)
Psychotria micrantha	Gap	12.3		295	41.7	12.4	9.1			Allen and Pearcy (2000)
Shorea multiflora	Gap	4.5							66.9	Cao and Booth (2001)
Vouacapoua Americana	Gap	7.2	42	88	81.8	29	8.4			Rijkers et al. (2000)
Castonopsis lamontii	Open	8.7	81.8	132.5	78.9	24.1	9.0	14.3		Present study
Isertia haenkeana	Open	19.5				27	6.1		33	Valladares et al. (1997)
Lithocarpus chingtungensis	Open	8.5	127	182	46.7	37	5.4	7.5	45.2	Unpublished data[a]
Manglietia insignis	Open	10.5	119	198	53.0	34.2	8.6	10.1	38.6	Unpublished data[a]
Group mean ± SD	Ust	4.0 ± 1.0	34.6 ± 12.5	78.6 ± 28.9	56.7 ± 13.3	35.1 ± 10.0	13.1 ± 8.1	17.9 ± 4.9	65.6 ± 7.1	
Group mean ± SD	Gap	7.9 ± 2.3	72.3 ± 57.5	178.9 ± 90.3	55.5 ± 17.7	24.6 ± 8.5	8.6 ± 1.2	no data	54.6 ± 15.4	
Group mean ± SD	Open	11.8 ± 5.2	109.3 ± 24.1	170.8 ± 34.1	56.3 ± 11.5	30.6 ± 6.0	7.3 ± 1.8	10.6 ± 3.4	38.9 ± 6.1	
Deciduous										

Table 4 continued

Species	Growth environment	A_{max} (μmol CO_2 m^{-2} s^{-1})	$g_{s\ initial}$ (mmol H_2O m^{-2} s^{-1})	$g_{s\ max}$ (mmol H_2O $m^{-2}s^{-1}$)	WUE_{max} (μCO_2 mol^{-1} H_2O)	IS_{1min} (%)	$t_{90\%A}$ (min)	$t_{90\%g}$ (min)	IS after 10 min shade (%)	Reference
Acer heptalobum	Ust	4.8	36.7	92.4	52.3	26.6	10.7	13.2	58.4	Unpublished data[a]
Acer rubrum	Ust	6.8	25	115	59.1		8.8	17.5	22[b]	Naumburg and Ellsworth (2000)
Acer rufinerve	Ust	2.8	56.9	102.6	27.6		9.9			Naramoto et al. (2001)
Fagus crenata	Ust	3.4	55.1	122.2	27.9		9.9			Naramoto et al. (2001)
Fagus lucida	Ust	5.1	49.8	110.1	47.5	21.3	11.1	14.8		Present study
Fagus sylvatica	Ust	4.3	15	90	47.8	5	11.5	12.9		Schulte et al. (2003)
Liquidambar styraciflua	Ust	6.4	22	106	60.4		25.6	40.6	67[b]	Naumburg and Ellsworth (2000)
Liriodendron tulipifera	Ust	5.7	46	110	51.8	46	9.4	17.1	61[b]	Naumburg and Ellsworth (2000)
Nothofagus cunninghamii	Ust	4.5	76	104	43.3	49	3.8	2.6		Tausz et al. (2005)
Styrax perkinsiae	Ust	4.6	65.7	124.3	36.7	38.6	7.9	9.4	44.6	Unpublished data[a]
Viburnum furcatum	Ust	2.8	53.2	82.3	34.5		5.3			Naramoto et al. (2001)
Acer rufinerve	Gap	8.1	48.9	167.7	48		14.7			Naramoto et al. (2001)
Fagus crenata	Gap	6.6	50.9	188.6	35.1		12.8			Naramoto et al. (2001)
Viburnum furcatum	Gap	6.0	43.3	133.9	44.7		11.1			Naramoto et al. (2001)
Acer heptalobum	Open	12.2	183	342	46.6	32.1	7.2	9.9	27.1	Unpublished data[a]
Fagus lucida	Open	9.7	146.5	272.5	35.6	25.6	8.1	10.5		Present study
Nothofagus cunninghamii	Open	8.0	123	167	47.9	77	1.5	1.1		Tausz et al. (2005)
Populus fremontii	Open						9.9			Roden and Pearcy (1993)
Populus tremuloides	Open						10			Roden and Pearcy (1993)
Styrax perkinsiae	Open	13.5	192	361	37.4	28.2	6.8	10.2	33.2	Unpublished data[a]
Group mean ± SD	Ust	4.7 ± 1.3	44.2 ± 18.9	105.4 ± 13.1	44.4 ± 11.5	28.1 ± 16.8	11.0 ± 5.4	16.0 ± 11.0	50.6 ± 17.9	
Group mean ± SD	Gap	6.9 ± 1.1	47.7 ± 3.9	163.4 ± 27.6	42.6 ± 6.7	no data	12.9 ± 1.8	No data	No data	
Group mean ± SD	Open	10.8 ± 2.5	161.1 ± 32.1	285.6 ± 87.8	39.2 ± 5.9	40.7 ± 24.3	7.3 ± 3.1	7.9 ± 4.6	30.2 ± 4.3	

Photosynthetic induction traits were generated from sudden increase of irradiance from low light ($\leq$20 μmol m^{-2} s^{-1}) to high light (above light-saturated point). Species within each phenological group are sorted according to growth environments

Ust forest understory, *Gap* forest gap, *Open* forest canopy or deforested open site

[a] The unpublished data were made by the authors in a montane humid evergreen broad-leaved forest in Ailao Mountain, Yunnan, southwestern China

[b] After 12 min shade instead

References

Allen MT, Pearcy RW (2000) Stomatal versus biochemical limitations to dynamic photosynthetic performance in four tropical rainforest shrub species. Oecologia 122:479–486

Boardman NK (1977) Comparative photosynthesis of sun and shade plants. Annu Rev Plant Physiol 28:355–377

Bowman DMJS, Prior LD (2005) Why do evergreen trees dominate the Australian seasonal tropics? Aust J Bot 53:379–399

Cai ZQ, Cao KF, Zheng L (2003) Photosynthetic induction in seedlings of six tropical rainforest tree species. Acta Phytoecol Sin 27(5):617–623 (in Chinese)

Cao KF (2001) Morphology and growth of deciduous and evergreen broad-leaved saplings under different light conditions in a Chinese beech forest with dense bamboo undergrowth. Ecol Res 16:509–517

Cao KF, Booth EB (2001) Leaf anatomical structure and photosynthetic induction for saplings of five dipterocarp species under contrasting light conditions in a Bornean heath forest. J Trop Ecol 17:163–175

Cao KF, Peters B, Oldeman RAA (1995) Climatic range and distribution of Chinese *Fagus* species. J Veg Sci 6:317–324

Chazdon RL (1988) Sunfleck and their importance to forest understory plants. Adv Ecol Res 18:1–63

Chazdon RL, Fetcher N (1984) Photosynthetic light environment in a lowland tropical rain forest in Costa Rica. J Ecol 72:553–564

Givnish TJ (1988) Adaptation to sun and shade: a whole plant perspective. Aust J Plant Physiol 15:63–92

Givnish TJ (2002) Adaptive significance of evergreen vs. deciduous leaves: solving the triple paradox. Silva Fenn 36(3):703–743

Han Q, Yamaguchi E, Odaka N, Kakubari Y (1999) Photosynthetic induction responses to variable light under field conditions in three species grown in the gap and understory of a *Fagus crenata* forest. Tree Physiol 19:625–634

Hendrickson L, Furbank RT, Chow WS (2004) A simple alternative approach to assessing the fate of absorbed light energy using chlorophyll fluorescence. Photosynth Res 82:73–81

Kirschbaum MUF, Pearcy RW (1988) Concurrent measurements of oxygen- and carbon dioxide exchange during lightflecks in *Alocasia macrorrhiza* (L.) G. Don Planta 174:527–533

Knapp AK, Smith WK (1989) Influence of growth forms on ecophysiological responses to variable sunlight in subalpine plants. Ecology 70:1069–1082

Kozaki A, Takeba G (1996) Photorespiration protects C_3 plants from photooxidation. Nature 384:557–560

Kramer DM, Johnson G, Kiirates O, Edwards GE (2004) New fluorescence parameters for the determination of Q_A redox state and excitation energy fluxes. Photosynth Res 79:209–218

Küppers M, Schneider H (1993) Leaf gas exchange of beech (*Fagus sylvatica* L.) seedlings in lightflecks: effects of fleck length and leaf temperature in leaves grown in deep and partial shade. Trees 7:160–168

Kursar TA, Coley PD (1993) Photosynthetic induction times in shade-tolerant species with long- and short-lived leaves. Oecologia 93:165–170

Leakey ADB, Scholes JD, Press MC (2005) Physiological and ecological significance of sunflecks for dipterocarp saplings. J Exp Bot 56:469–482

Liu S, Robert OT (1995) Responses of foliar gas exchange to long-term elevated CO_2 concentration in mature loblolly pine trees. Tree Physiol 15:351–359

Logan BA, Barker DH, Adams WW III, Demmig-Adams B (1997) The response of xanthophyll cycle-dependent energy dissipation in *Alocasia brisbanensis* to sunflecks in a subtropical rainforest. Aust J Plant Physiol 24:27–33

Lovelock CE, Kursar TA, Skillman JB, Winner K (1998) Photoinhibition in tropical understory species with short-and long-lived leaves. Funct Ecol 12:553–560

Miyake C, Yokota A (2001) Cyclic flow of electrons within PSII in the thylakoid membranes. Plant Cell Physiol 42:508–515

Naramoto M, Han Q, Kakubari Y (2001) The influence of previous irradiance on photosynthetic induction in three species grown in the gap and understory of a *Fagus crenata* forest. Photosynthetica 39(4):545–552

Naumburg E, Ellsworth DS (2000) Photosynthetic sunfleck utilization potential of understory saplings growing under elevated CO_2 in FACE. Oecologia 122:163–174

Ögren E, Sundin U (1996) Photosynthetic responses to variable light: a comparison of species from contrasting habitats. Oecologia 106:18–27

Öquist G, Anderson JM, McCraffery S, Chow WS (1992) Mechanistic differences in photoinhibition of sun and shade plants. Planta 188:422–431

Osmond CB, Grace SC (1995) Perspectives on photoinhibition and photorespiration in the field: quintessential inefficiencies of the light and dark reactions of photosynthesis? J Exp Bot 46:1351–1362

Pearcy RW (1983) The light environment and growth of C_3 and C_4 tree species in the understory of a Hawaiian forest. Oecologia 58:19–25

Pearcy RW (1987) Photosynthetic gas exchange responses of Australian tropical forest trees in canopy, gap and understory micro-environments. Funct Ecol 1:169–178

Pearcy RW (1990) Sunflecks and photosynthesis in plant canopies. Annu Rev Plant Physiol Plant Mol Biol 41:421–453

Peek MS, Russek-Cohen E, Wait DA, Forseth IN (2002) Physiological response curve analysis using nonlinear mixed models. Oecologia 132:175–180

Poorter L, Oberbauer SF (1993) Photosynthetic induction responses of two rainforest tree species in relation to light environment. Oecologia 96:193–199

Rijkers T, Vries PJ, Bongers PF (2000) Photosynthetic induction in saplings of three shade-tolerant tree species: comparing understory and gap habitats in a French Guiana rain forest. Oecologia 125:331–340

Roden JS, Pearcy RW (1993) Photosynthetic gas exchange response of poplars to steady-state and dynamics light environments. Oecologia 93:208–214

Schulte M, Offer C, Hansen U (2003) Induction of CO2-gas exchange and electron transport: comparison of dynamic and steady-state responses in *Fagus sylvatica* leaves. Trees 17:153–163

Stegemann J, Timm HS, Küppers M (1999) Simulation of photosynthetic plasticity in response to highly fluctuating light: an empirical model integrating dynamic photosynthetic induction and capacity. Trees 14:145–160

Tang YH, Hiroshi K, Mitsumasa S, Izumi W (1994) Characteristics of transient photosynthesis in *Quercus serrata* seedlings grown under lightfleck and constant light regimes. Oecologia 100:463–469

Tausz M, Warren CR, Adams MA (2005) Dynamic light use and protection from excess light in upper canopy and coppice leaves of *Nothofagus cunninghamii* in an old growth, cool temperate rainforest in Victoria, Australia. New Phytol 165:143–156

Valentini R, Epron D, de Angelis P, Matteucci G, Dreyer E (1995) In situ estimation of net CO_2 assimilation, photosynthetic electron flow and photorespiration in Turkey oak (*Q. cerris* L.) leaves: diurnal cycles under different leaves of water supply. Plant Cell Environ 18:631–640

Valladares F, Allen MT, Pearcy RW (1997) Photosynthetic responses to dynamic light under field conditions in six tropical rainforest shrubs occurring along a light gradient. Oecologia 111:505–514

Watling JR, Robinson SA, Woodrow IE, Osmond CB (1997) Responses of rainforest understory plants to excess light during sunflecks. Aust J Plant Physiol 24:17–25

Zar JH (1984) Biostatistical analysis. Prentice Hall, Englewood Cliffs

Zipperlen SW, Press MC (1997) Photosynthetic induction and stomatal oscillations in relation to the light environment of two dipterocarp rain forest tree species. J Ecol 85:491–503